

***Far-Infrared Study of Two-Dimensional
Air-Rod Photonic Crystals
—Band Gap, Uncoupled Mode and Wavevector Mismatch—***

Yoshiyuki DOI, Noriko KAWAI and Mitsuo WADA

Department of Physics, Faculty of Science, Shinshu University, Matsumoto 390, Japan

(Received 28th January 1997)

Abstract

Two-dimensional photonic crystals both of square and triangular lattices composed of circular air-rods with the lattice constant of $170 \mu\text{m}$ were fabricated. The photonic band structures were studied by far-infrared transmission measurements. The clear opaque regions due to the band gap and due to the non coupling between photonic mode and external wave were observed in both lattices. The uncoupled modes can not be excited by an external mode because their wave functions are anti-symmetric under the relevant mirror reflection defined on the lattice. Furthermore, some regions with very low transmittance were found, where exist only a band whose dominant plane-wave component in eigen-function has wavevector not parallel to the propagating direction of the external incident wave. These low transmittance are considered to be caused by wavevector mismatch between photonic modes and external incident waves. The observed spectra are discussed compared with the results of band structure calculated by means of a plane-wave expansion method as well as of the symmetry consideration.

1 Introduction

The optical properties of periodic dielectric structures, which are called photonic crystals or photonic lattices, have been attracting much attention.¹⁻¹⁶ The main reason for the recent intensive investigation is that a frequency range where no propagating electromagnetic mode exists can realised by means of the proper choice of the lattice structure and the dielectric constants. This frequency region is called a photonic band gap. When we emphasise the fact that the propagation of the electromagnetic wave is forbidden along all three-dimensional (3D)²⁻⁴ or two-dimensional (2D)¹⁷⁻¹⁸ directions for any polarization, we call it an absolute or complete gap. Those lattice with a band gap are expected to open the door to a new field in quantum optics. Since electromagnetic modes with frequencies in the absolute gaps are totally absent, spontaneous emission is forbidden in situations where the band gap overlaps the

electronic band edge. The inhibition of spontaneous emission can improve the performance of many optoelectronic devices such as semiconductor lasers with high efficiency. The absence of electromagnetic modes in a certain frequency range can also modify the basic properties of many atomic, molecular and excitonic systems and bring enhancement of non-linear optical effects.^{15,16} For these purposes, development of a lattice with the gap frequency at visible and near-infrared region is inevitably important. However, those lattice are technically very difficult to fabricate at present.^{19–22} The development of new fabrication strategies to scale the features of spectrum into the visible or near-infrared regime and of novel applications is one of goal of present experimental studies.

On the view point of fabrication techniques the 2D structure will be desirable compared with 3D ones even by growing it layer by layer using conventional lithograph techniques in the near future. Recently, Inoue et al. reported a comparison of the photonic band gap profiles between two similar 2D air-rods triangular lattices fabricated with the respective lattice constant of $1.02 \mu\text{m}$ and $1.17 \mu\text{m}$.^{23,24} These were fabricated by means of the technology for producing microchannel plates. Transmission spectra in the near-infrared region relevant to the gap have revealed that the respective non-transmission wavelength regions are observed with the expected relative shift between two lattices, for E and H polarization for which electric or magnetic vector is parallel to the axis of air-rods, respectively. The calculation of band structure of 2D lattice is remained in the employing a scalar wave equation. The absolute values and relative position of band gap frequencies were revealed by the calculation based on the plane wave expansion. They showed good agreement. These results indicate that the observed non-transmission region arise from photonic band gap, and thus a absolute gap exists for H polarization.

The existence of non-coupling between photonic mode and the incident external wave was first pointed out by Robertson *et al.*¹³ Based on the observation of the dispersion relation for a 2D square lattice of circular dielectrics-rods by their coherent microwave transient spectroscopy technique, they argued that the anti-symmetric modes under the mirror reflection at the plane spanned by the incident wavevector and the z axis (perpendicular to the 2D plane) do not couple to the incident plane wave at normal incidence because the latter is symmetric under the same mirror reflection, and hence, the effective coupling between them is absent. They derived the same conclusion for photonic bands in a particular direction in a 2D triangular lattice of dielectrics-rods as well. The existence of uncoupled mode was also pointed out by Sakoda based on the numerical calculation of the transmission spectra for a 2D triangular lattice of circular air-rods.^{25,26} It was shown that there was an opaque frequency range in spite of its non-zero state density and this fact was interpreted as originating from the non-coupling between the internal mode and the external plane wave. From the group

theoretical classification of photonic bands in the 2D triangular and square lattices, he pointed out that here exist several uncoupled modes.

In the previous paper we reported the comparison of the observed transmission spectra with the transmittance and band structure calculated by plane-wave expansion method and confirmed the uncoupled mode in a 2D photonic lattice with the lattice constant of $170\mu\text{m}$ composed of a triangular array of circular air-rods with diameter of $105\mu\text{m}$.²⁷ The comparison of observed transmission spectra in far-infrared region with the calculated band structure gave clear evidence for the existence of the uncoupled mode along the Γ - J direction for E polarization. The existence of an uncoupling mode was also confirmed by the numerical calculation of transmittance by means of the plane wave expansion method.

In the present paper we will report the details of the polarization and direction dependencies of the transmission spectra observed both in the square and triangular lattices, and discuss the profiles on the basis of symmetry consideration and on comparison with the dispersion relations calculated by means of the plane wave expansion method.

2 Experimental Procedures

2-1 Fabrication of photonic lattices

In the present specimens both of the square and triangular lattices, the circular air-rod holes were made by direct drilling into methylpentene polymer (Mitsui Oil Chemicals, TPX) plates by means of a numerically controlled (NC) milling machine (see Fig. 1 (a)). TPX polymer was chosen because it is transparent and lossless in the far-infrared range, its dielectric constant 2.1 is relatively large among the polymers and it does not show frequency dependence in the relevant range. The lattice is consisted of 35×35 holes in the square lattice specimen measured for Γ - X direction and 31×31 holes for Γ - M direction, respectively, and 30×30 cylindrical holes in the triangular lattice specimen. To make long distance holes with small radius parallel each other into the polymer material is quite hard, so that we made the similar ten plates with the thickness along the air-rod hole axis of 0.5mm . Then they are stacked as their holes agree in position each others by use of four metal guide pins at each corner. The effective cross section of the specimens thus fabricated was about $5\times 5\text{mm}^2$. The front and rear surface were polished to be optically flat. The lattice constant and the diameter of the holes were determined by direct observation of an optical microscope and they are $170\pm 3\mu\text{m}$ and $95\pm 15\mu\text{m}$ in the square lattice and $170\pm 3\mu\text{m}$ and $105\pm 15\mu\text{m}$ in the triangular lattice, respectively. The refractive index of TPX was 1.46 ± 0.02 around 30cm^{-1} ($\lambda = 333.3\text{mm}$, $\nu = 900\text{GHz}$), which was estimated from the period of interference wave like pattern on the transmission spectrum of a thin film of TPX prepared from the same block from which the photonic lattice plates were

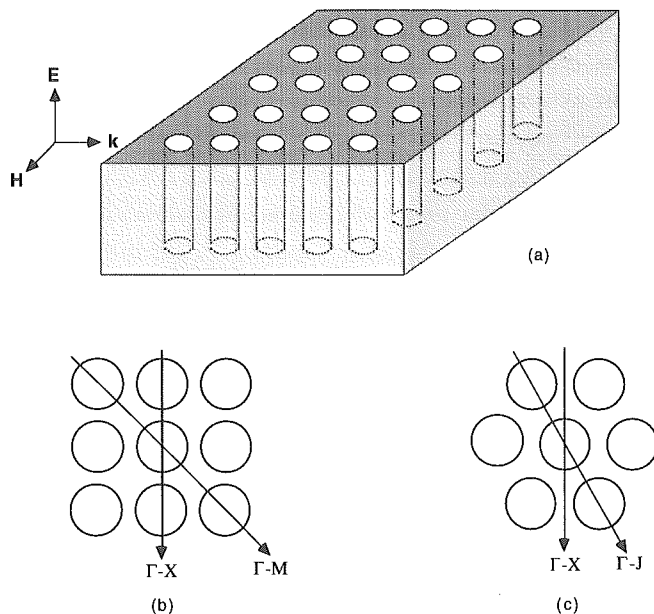


Fig. 1 Schematic of 2D lattice composed of parallel air cylinders (a) and cross-sectional geometries of square (b) and triangular (c) lattice, where the respective high-symmetry directions are shown.

made. The pattern dues to the interference between waves directly transmitting and those transmitting after reflected the rear and front surface of thin films.

2-2 Far-infrared transmission measurements

The transmission spectra were measured with a Fourier transform infrared spectrometer (JASCO, FT/IR MW7900) in Martin-Puplett configuration with three free-standing tungsten wire-grid polarizers as a beam splitter, a polarizer and an analyzer. The details of the spectrometer is described fully in the ref. 29. A water-cooled high-pressure mercury lamp was used as a far-infrared radiation source. The incident far-infrared wave was focused on the sample with a parabolic concave mirror with a focal length of 150 mm and an effective diameter of 45mm ($F=3.3$). The transmitted wave was detected with a Si : Ga composite bolometer cooled in a liquid He cryostat that was placed at the optical configuration symmetric with the incident side. The NEP (noise equivalent power) of the bolometer is below $3 \times 10^{-15} \text{ W}/\sqrt{\text{Hz}}$. The spectra from 5cm^{-1} to 120cm^{-1} were measured at room temperature with the minimum spectral resolution of 0.25cm^{-1} . The transmission spectra propagating along both $\Gamma-X$ and $\Gamma-M$ directions were measured for the polarization H and E in the square lattice specimen (see Figs. 1 (b) and 1 (c)). In the triangular lattice the spectra along $\Gamma-X$ and $\Gamma-J$ directions for H and E polarizations were observed.

3 Photonic Band Structure

3-1 Square lattice

There exist two kinds of polarization for the photonic states propagating in 2D lattices. The E polarization corresponds to states with the electric field parallel to the air-rods axes. So, the magnetic field lies in the lattice plane and is odd under the reflection in this plane. In the case of H polarization, the electric field is parallel to the lattice plane and invariant in the reflection. In order to classify the photonic states at the three high symmetry point of Brillouin zone in the squarer lattice, we must consider the irreducible representations of k group at the Γ , M and X points, whose

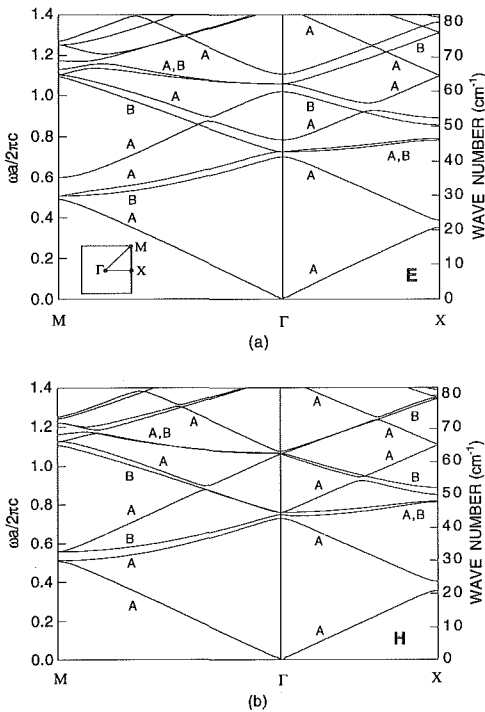


Fig. 2. Photonic band structure of 2D square lattice composed of cylindrical holes formed in TPX for (a) E polarization and (b) H polarization. Following parameters were assumed: the lattice constant is $170 \mu\text{m}$, the hole diameter is $95 \mu\text{m}$, and the dielectric constant of TPX is 2.1. The ordinate on the left side is the normalised frequency, where a is the lattice constant and c the light velocity in vacuum.

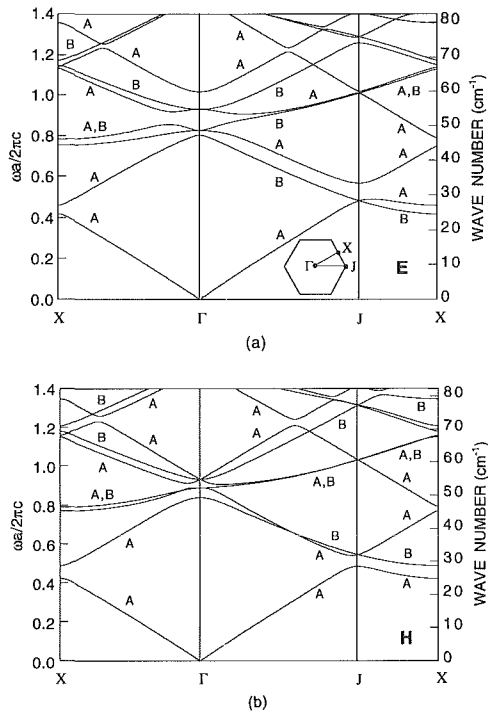


Fig. 3. Photonic band structure of 2D triangular lattice composed of cylindrical holes formed in TPX for (a) E polarization and (b) H polarization. Following parameters were assumed: the lattice constant is $170 \mu\text{m}$, the hole diameter is $105 \mu\text{m}$, and the dielectric constant of TPX is 2.1. The ordinate on the left side is the normalised frequency, where a is the lattice constant and c the light velocity in vacuum.

wavevector is $(0, 0)$, $2\pi/a(1/2, 0)$, and $2\pi/a(1/2, 1/2)$, where a is the lattice constant and we took the elementary lattice vectors as $(a, 0)$ and $(0, a)$, respectively. Because the dielectric constant of TPX is not very large, and hence, the dispersion relation is not very far from that in the empty lattice, we can assign a corresponding irreducible representation to each band of the actual lattice. Only one mirror reflection is defined on segment Γ - X and segment Γ - M because of their low symmetry. The wave function of mode A on segment Γ - M (Γ - X) is symmetric under the mirror reflection at the plane which includes the segment Γ - M (Γ - X) and perpendicular to the lattice plane, whereas that of mode B is anti-symmetric under the same mirror reflection.

The band structure of the photonic crystal with circular air-rod square lattice of TPX was calculated by the plane-wave expansion method according to Plihal and Maradudin¹⁸ with 289 basis plane-waves as mentioned in the previous paper.²⁵ The lattice constant a is 170 μm , the diameter of the circular rod is 95 μm , and the dielectric constant of methylpentene polymer (TPX) is 2.1. Figures 2 (a) and 2 (b) show the calculated band structures (a) for H polarization and (b) for E polarization, respectively. The mode assignment is also shown in these Figures, where notation as A, B means that the assignment is not rigorously determined by the knowledge of the group theory alone.²⁶ In these figures, the gap between the first and the second bands is seen around 22cm^{-1} for both polarizations of Γ - X direction and around 30cm^{-1} for both polarizations of Γ - M direction. We again find several frequency ranges where only a B mode exists, where we expect a total reflection and a non-transmission as before. For instances, we find the frequency ranges around 56cm^{-1} for both polarizations of the Γ - X direction and those around 52cm^{-1} for both polarizations of the Γ - M direction (Table II).

3-2 Triangular lattice

Next, we examine the case of triangular lattice. There exist the three high symmetry points of Brillouin zone of the triangular lattice, i.e., the Γ , J and X points, whose wave vector is $(0, 0)$, $(2\pi/a)(2/3, 0)$, and $(2\pi/a)(1/2, 1/2\sqrt{3})$, where a is the lattice constant and we took the elementary lattice vectors as $(a, 0)$ and $(a/2, 3a/2)$, respectively. The eigen frequencies were calculated for plane wave in the empty lattice as before. The notation of the mode A and B is the same as before, i.e., the wave function of mode A on segment Γ - J (Γ - X) is symmetric under the mirror reflection at the plane which includes the segment Γ - J (Γ - X) and is perpendicular to the lattice plane, whereas that of mode B is anti-symmetric under the same mirror reflection.

Figures 3(a) and 3(b) show the dispersion relations calculated with 289 basis plane-waves, as well as the mode assignment, (a) for H and (b) for E polarization, respectively. The dielectric constant of the circular rod and the background material were also assumed to be 1.0 and 2.1, respectively. The lattice constant was taken as 170

μm , and the diameter of rod hole as $105 \mu\text{m}$. In these figures, we find a gap between the first and the second lowest bands at the X point for both polarizations. We also find a gap at the J point for H polarization. On the other hand, there is no band gap for E polarization because the corresponding two bands are degenerate. The band gap frequencies are listed in Table I. As for the uncoupled mode, we find that the second lowest band along the Γ - J direction for E polarization is the B mode. The wave function of this mode is anti-symmetric under the mirror reflection mentioned above, and it does not couple to external plane-wave at normal incidence. In the region corresponding to the frequencies between the first and the second bands at J point the incident radiation is reflected completely and does not transmit. We also find that there are several other frequency ranges where only a B mode exists. The frequencies of opaque region due to the non-coupling are listed in the Table II.

4 Far-Infrared Transmission Spectra

4-1 Square lattice

Figures 4 (a) and 4 (b) show the transmission spectra observed in the configurations propagating Γ - X and Γ - M directions for H and E polarizations, respectively. Now let us see the spectra of Γ - X direction as the order of wave number. First, we can see the sharp dip around 22 cm^{-1} for both H and E polarizations. Those dips correspond to the gaps between the lowest band and second lowest band in Γ - X direction. Next, we have a very wide regions with low transmittance from 41 to 47 cm^{-1} for E polarization whereas for H polarization the relatively narrow dip is seen around 44 cm^{-1} . These origin will be discussed in the following section. We can see almost opaque regions around 56 cm^{-1} for both polarizations which correspond the gaps between the fourth and fifth band belonging to the A representation, where only the anti-symmetric B band exists which can not coupled with external wave.

Next, In the spectra of Γ - M direction, it is seen that a wide region from 29 cm^{-1} to 37 cm^{-1} shows very low transmittance for E polarizations. The width of the band gap between the first and second band of Γ - M direction for E polarization is estimated 2 cm^{-1} around 30 cm^{-1} estimated from the dispersion curves. On the other hand, for the H polarization almost opaque region is seen from 30 cm^{-1} to 33 cm^{-1} . The observed width of region is 3 cm^{-1} in spite that the value estimated from dispersion curves is only 1 cm^{-1} . These reasons are considered in the next section. The dips around 52 cm^{-1} seen for both polarizations correspond to the gaps between the third and the fourth A band where the only uncoupled second B band exists in Γ - M direction. The very low transmittance region observed from 59 cm^{-1} to 67 cm^{-1} for E polarization also will be discussed in the following section.

We can see relatively large dip around 30 cm^{-1} in the spectrum for H polarization of Γ - X direction. This dip may be due to the interference between the front and rear

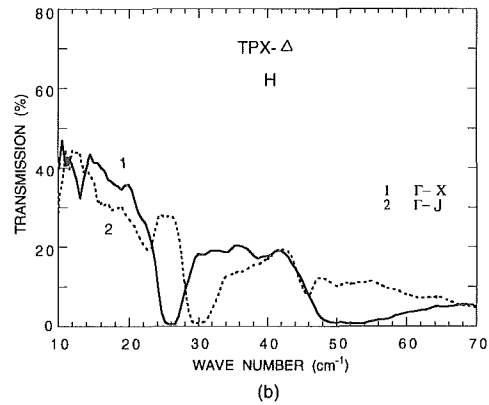
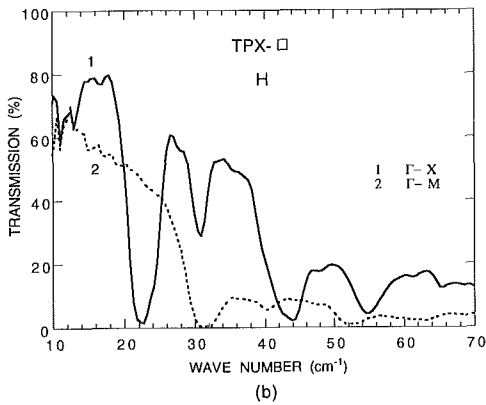
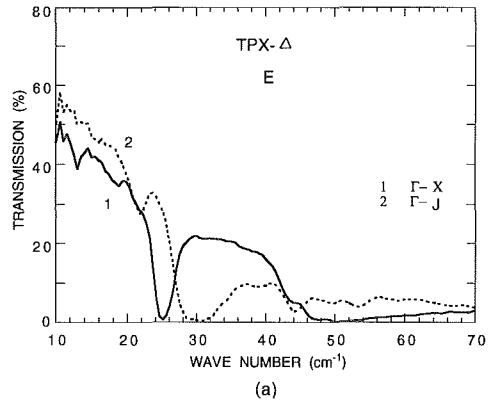
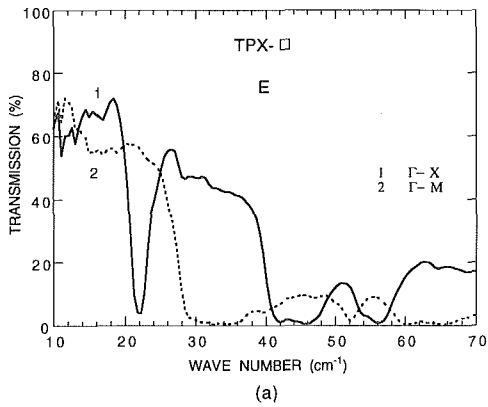


Fig. 4. Transmission spectra of the 2D square lattice observed (a) for E polarization and (b) for H polarization of the $\Gamma-X$ and $\Gamma-M$ directions. The specimen was composed of cylindrical holes formed in a TPX with lattice constant of $170 \mu\text{m}$ and the average hole diameter of $95 \mu\text{m}$.

Fig. 5. Transmission spectra of the 2D triangular lattice observed (a) for E polarization and (b) for H polarization of the $\Gamma-X$ and $\Gamma-J$ directions. The specimen was composed of cylindrical holes formed in a TPX (methylpentene polymer) with lattice constant of $170 \mu\text{m}$ and the average hole diameter of $105 \mu\text{m}$.

surface of specimen.

4-2 Triangular lattice

The typical transmission spectra for H and E polarizations along the both $\Gamma-X$ and $\Gamma-J$ directions observed are shown Figs. 5(a) and 5(b), respectively. In these figures, we find opaque frequency ranges with transmittance less than 2% around 25 cm^{-1} for both polarization of $\Gamma-X$ direction, and around 30 cm^{-1} for both polarizations of $\Gamma-J$ direction. These opaque regions observed for H and E of $\Gamma-X$, and for H of $\Gamma-J$ correspond to the gap frequency between the lowest and the second lowest bands

which are listed in Table I. On the other hand, that observed for E of Γ - J corresponds to the region where there exists only uncoupled mode mention above. Furthermore, we can see the broad dips around 50 cm^{-1} in the spectra for both H and E polarizations of Γ - X direction. Those regions correspond to the gap between the fourth and fifth bands for both H and E polarizations of Γ - X direction. However, the widths of low transmittance ranges observed are wider than those estimated from dispersion curves. We will discuss those regions in the next section.

Other fine structures are seen, for examples, dips around 22 cm^{-1} for both polarizations of Γ - J direction, 46 cm^{-1} for H of Γ - J , and 44 cm^{-1} for E of Γ - J . We can not interpret these dips only from the dispersion curves. These dips may due to the interference between the front and rear surface of specimen. The all transmittance observed show the trend of decrease with increasing wave number. The reason is not clear at present, however the next two reasons are suspected, (i) the energy flow to the transverse direction due to the limited number of unit cell, and (ii) the low mechanical accuracy of side surfaces of air-rod holes caused by thermal deformation during the mechanical drilling process. However, this trend does not affect the discussion of the present study effectively, so that we do not take into account any more.

5 Discussions

In this study we found the quite low transmittance region in the observed transmission spectra of 2D photonic crystals with both air-rod triangular and square lattices. From the comparison with dispersion relations, the reasons of low transmittance are classified the following three origins: (1) band gap, (2) uncoupled mode, and (3) others. We will discuss firstly the photonic band gap and next uncoupled mode. Finally we will discuss that the wavevector mismatch dues to the third reason of the very low transmittance observed.

5-1 Band gap

In the square lattice the gap between the first and second band (first gaps) are expected from the dispersion curve of Figs. 2 (a) and 2 (b), and they are clearly observed

TABLE I. Comparison of the first gap frequencies between observation and calculation in the square and triangular lattices.

polarization	square lattice		triangular lattice	
	Γ - X	Γ - M	Γ - X	Γ - J
E exp.	21.5-22.5	—	24.5-26.3	—
E cal.	21.0-23.0	—	24.6-27.0	—
H exp.	21.5-22.5	—	24.6-27.6	28.5-31.6
H cal.	20.6-23.5	—	24.8-28.6	28.4-32.0 (cm^{-1})

around 22 cm^{-1} both for H and E polarizations of Γ - X direction as seen in Figs. 4 (a) and 4 (b). Both for H and E polarization of the Γ - M direction in the square lattice, the upper side edge frequencies of first gaps around 30 cm^{-1} are not clear because the regions due to other reason of low transmittance connect the upper edge of the first band gaps. In the band gaps between the second and the third lowest band for both polarization of Γ - X direction in the square lattice around 42 cm^{-1} , the upper edge frequency of gap is also connected by the regions due to other reason of low transmittance. Those cases will be discussed in the subsection ⁵⁻³

In the triangular lattice the gaps between the first gap are clearly observed around 25 cm^{-1} both for H and E polarizations of Γ - X direction, and around 30 cm^{-1} for H polarization for Γ - J direction as seen in Figs. 5 (a) and 5 (b) as expected from the calculation results of Figs. 3 (a) and 3 (b). In the case of the gap between the fourth and fifth lowest bands for both polarizations of Γ - X direction in the triangular lattice the band gap frequency is overlapped the region due to other reason of low transmittance. The comparison of the gap frequency between observation and calculation shows quite excellent agreement in both lattices and listed in Table I.

5-2 Uncoupled mode

Next, we will discuss the opaque regions due to the non-coupling effect. The opaque regions where exist the only modes belonging to the B irreducible representation which can not be excited by the incident external plane wave are observed. In the square lattice, we can expect those regions around 55 cm^{-1} for both polarization of Γ - X direction and around 52 cm^{-1} for both polarizations of Γ - M direction from the calculated dispersion curves in Fig. 2. As seen in Fig. 4, we can confirm the low transmittance regions at the corresponding frequencies. The comparison between observation and calculation is listed in Table II.

In the triangular lattice we have already reported that the opaque region observed from 22 cm^{-1} to 33 cm^{-1} for E polarization of Γ - J direction dues to the non-coupling of the second band belonging to the anti-symmetric B representation as shown in

TABLE II. Comparison of frequency ranges related to the non-coupling between observation and calculation in the square and triangular lattices.

polarization	square lattice		triangular lattice	
	Γ - X	Γ - M	Γ - X	Γ - J
E exp.	55.0-57.0	51.5-52.5	—	28.0-33.0
E cal.	56.5-57.5	52.0-53.5	—	28.4-33.4
H exp.	54.0-55.0	51.0-53.0	—	—
H cal.	55.0-56.0	52.0-53.5	—	— (cm ⁻¹)

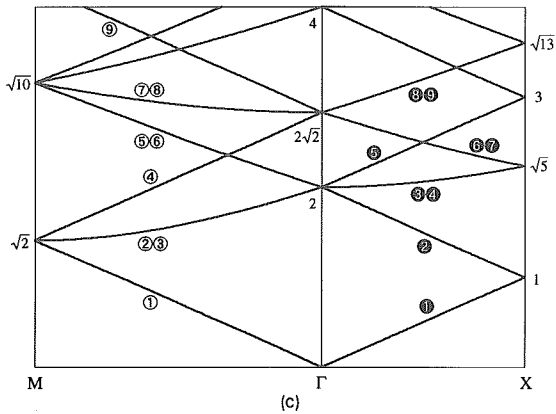
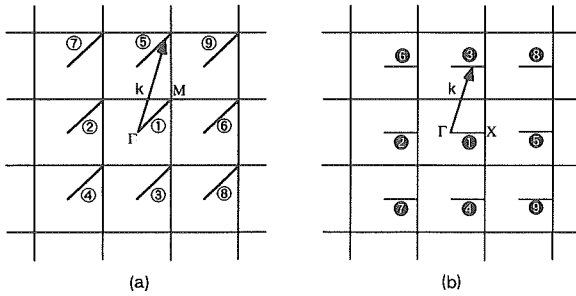


Fig.6. Photonic band structure of 2D hypothetical square lattice in vacuum (empty lattice) (c) and corresponding branches in Brillouin zone for Γ - M (a) and Γ - X (b), where $\Gamma=(0,0)$, $X=(2\pi/a)(1/2,0)$, and $M=(2\pi/a)(1/2,1/2)$.

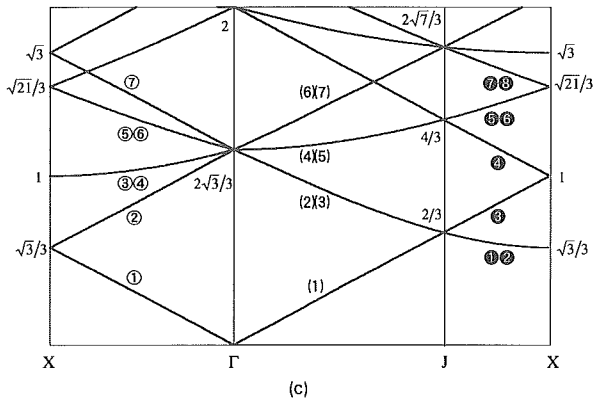
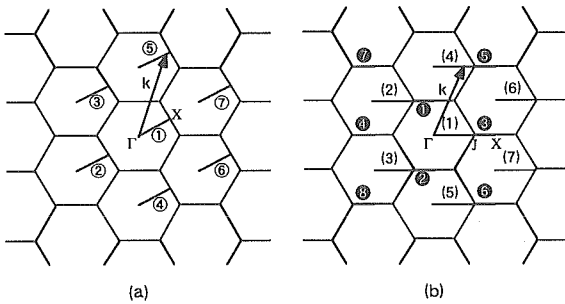


Fig.7. Photonic band structure of 2D hypothetical triangular lattice in vacuum (empty lattice) (c) and corresponding branches in Brillouin zone for Γ - X (a) and Γ - J - X (b), where $\Gamma=(0,0)$, $X=(2\pi/a)(1/2\sqrt{3},0)$, and $J=(2\pi/a)(2/3,0)$.

Figs. 5 (b) and 4 (b). This fact can be clearly demonstrated by numerical calculation of the transmission spectra by the plane wave expansion method.²⁷ The correspondence between this frequency range and the calculated opaque range is quite good as shown in Table II.

5-3 *Wavevector mismatch*

Finally, we will discuss other regions with very low transmittance in spite that in this region there exists the photonic mode belonging to the A representation, that is, the same symmetry as that of incident wave. As mentioned in the previous section we find these kinds of region both in square and triangular lattices.

Quite recently, *H. Miwa* indicates that the contribution to the transmittance must be small from the A mode whose wavevector of dominant plane-wave component in eigen-function is not parallel to that of incident external wave in the photonic lattice of the small dielectric constant rate.³⁰ Transmittance (reflectance) of a wave through a boundary of two media is determined by matching among the incident, reflected and transmitted waves throughout the surface of the boundary. In the case of the normal incidence (with infinite aperture) to a planar surface of the photonic crystal, the wave vector of the incident wave has no components along the plane. In the low frequency region, where no Bragg reflection is allowed, the wave vector of the reflected wave neither has components along the plane. When the eigen-function of the photonic mode is expanded in plane waves, only plane-wave components with wave vector parallel to that of the incident wave (perpendicular to the surface) can meet the above matching condition. Other plane-wave components of the mode should be matched with surface waves, which are localised in the vicinity on the both side of the boundary surface. For the TPX photonic crystals, where the ratio of the dielectric constants is not far from unity, the correspondence of the photonic band to that for the empty lattice is very good both in eigen-frequencies and eigen-functions. Thus, if only one photonic mode with the relevant symmetry (A representation) exists for the incident frequency, we can expect the best matching and high transmittance for those branches of the photonic mode, which correspond to the plane wave in the empty lattice with wave vectors parallel to the incident wave, whereas poor matching and low transmittance for those branches corresponding to wave vectors with different directions. In the following we call the latter situation as "wavevector mismatch".

Thus, we must attract our attention to the direction of wavevector of dominant plane-wave component in eigen-function of each band. Figs. 6 and 7 show photonic band structure of 2D hypothetical triangular and square lattices in vacuum (empty lattice) and corresponding branches in Brillouin zone. Firstly, we will consider the case of the square lattice. As seen in Fig. 4, in the Γ - X direction we have a very wide regions with low transmittance from 41 to 47 cm^{-1} for E polarization whereas for H

polarization the narrow dip is seen around 44 cm^{-1} . From the dispersion curves as shown in Fig.2 and Figs 6 (b) and 6 (c), we can see this frequency range may correspond to the frequency range between the second and fifth bands where exist two bands one of which belongs to the A representation. The external incident wave propagates along the direction parallel to Γ - X , that is, parallel to the direction from $(0,0)$ to $(2\pi/a)(1/2,0)$. The wavevectors of dominant plane-wave components in eigen-functions of the second and fifth bands are on the line from $(2\pi/a)(-1,0)$ to $(2\pi/a)(-1/2,0)$ and $(2\pi/a)(1,0)$ to $(2\pi/a)(3/2,0)$, respectively, so that they are parallel to that of the incident wave. On the other hands, those of the third and fourth bands are on the line from $(2\pi/a)(0,1)$ to $(2\pi/a)(1/2,1)$ or $(2\pi/a)(0,-1)$ to $(2\pi/a)(1/2,-1)$ (in the empty lattice the third and fourth bands are completely degenerate as shown in Fig. 6 (c)). That is, the dominant plane-wave components in eigen-function of the third and the fourth bands have the wavevectors not parallel to that of the incident external wave. Therefore the contribution of the third or the fourth band (one of which is uncoupled mode) to the transmittance should be small, so that the frequency range between the second and the fifth bands appears to be almost opaque region in the transmission spectra. For the E polarization the region with low transmission is expected to be wider than that for H polarization from dispersion curves and this fact can be confirmed by observed spectra (Fig. 4). The small peak seen around 43 cm^{-1} may come from the high density of state because that the dispersion curve of the relevant band is almost flat.

In the spectra of Γ - M direction, it is found that a wide region from 29 to 37 cm^{-1} has very low transmittance for E polarizations as shown in Fig. 4 (a). From the dispersion curves of Figs. 2 (a), the opaque region is expected in the range between the first and third bands. The width of the band gap between the first and third bands of Γ - M direction for E polarization is estimated 2 cm^{-1} around 30 cm^{-1} from the dispersion curves in Fig. 2 (a). For the H polarization almost opaque region is seen around 30 cm^{-1} . The observed width of region is 4 cm^{-1} in spite that the value estimated from dispersion curves in Fig. 2 (b) is only 1 cm^{-1} . These profiles can be explained by the similar augment of wavevector mismatch discussed above. These regions correspond to the frequency range between the first and the fourth band for both polarization of Γ - M direction. The external incident wave propagates along the direction parallel to Γ - M . The wavevectors of dominant plane-wave component in eigen-functions of the first and fourth bands are on the line from $(0,0)$ to $(2\pi/a)(1/2,1/2)$ and $(2\pi/a)(-1,-1)$ to $(2\pi/a)(-1/2,-1/2)$, respectively, so that they are parallel to that of the incident external wave (Figs. 6 (a) and 6 (c)). Whereas, those of the second and third bands are on the line from $(2\pi/a)(-1,0)$ to $(2\pi/a)(-1/2,1/2)$ and $(2\pi/a)(0,-1)$ to $(2\pi/a)(1/2,-1/2)$ so that they are not parallel to that of incident external wave. The contribution of the third band to the transmittance should be small and the second band is the uncoupled mode. Therefore the frequency range between the first and the fourth bands

TABLE III. Comparison of frequency ranges related to the wavevector mismatch between observation and calculation in the square and triangular lattices.

polarization	square lattice			triangular lattice	
	Γ - X	Γ - M		Γ - X	Γ - J
E exp.	41.0-47.0	29.0-37.0	59.0-68.0	53.5-59.6	—
E cal.	42.5-46.8	29.3-35.0	61.0-67.0	51.1-63.7	—
H exp.	42.5-43.5	30.0-33.0	small dip	49.0-56.0	—
H cal.	43.0-45.0	29.5-33.0	63.0-64.0	53.5-59.6	— (cm ⁻¹)

is observed as the low transmission region. For the E polarization the region with low transmission is expected to be wider than that for H polarization from the estimation of dispersion curves and this fact can be also confirmed by observed spectra. The very low transmittance region observed from 59 to 67 cm⁻¹ for E polarization also corresponds to the frequency range between the sixth and ninth bands. This region is also explained by the wavevector mismatch and non-coupling effect.

Next, we will consider the case of triangular lattice. In the spectra for both polarization for Γ - X direction we can find very low transmittance region from 49 cm⁻¹ to 55 cm⁻¹ (Fig. 5). From the dispersion curves as shown in Fig. 3 we can see this frequency range should be correspond to the frequency range between the second and seventh lowest bands where exist four bands including two bands belonging to the A representation (the fourth and the fifth lowest bands). The external incident wave propagates along the direction parallel to Γ - X , that is, parallel to the direction from (0,0) to $(2\pi/a)(1/2, 1/2\sqrt{3})$. The wavevectors of dominant plane-wave components in eigen-functions of the first and the second lowest bands are on the line from (0,0) to $(2\pi/a)(1/2, 1/2\sqrt{3})$ and from $(2\pi/a)(-1, -1/\sqrt{3})$ to $(2\pi/a)(-1/2, -1/2\sqrt{3})$, so that they are parallel to that of incident wave. The wavevector of the dominant plane-wave components in eigen-functions of the seventh band is on the line from $(2\pi/a)(1, 1/\sqrt{3})$ to $(2\pi/a)(3/2, \sqrt{3}/2)$, so that it is also parallel to the that of incident wave. Whereas, the those in eigen-function of the fourth and fifth bands have the wavevectors not parallel to that of the incident external wave. The wavevectors of the fourth band are oriented to the direction along the line from $(2\pi/a)(0, -2/\sqrt{3})$ to $(2\pi/a)(1/2, -\sqrt{3}/2)$ and from $(2\pi/a)(-1, 1/\sqrt{3})$ to $(2\pi/a)(-1/2, \sqrt{3}/2)$ and those of the fifth band are from $(2\pi/a)(1, -1/\sqrt{3})$ to $(2\pi/a)(3/2, -1/2\sqrt{3})$ and from $(2\pi/a)(0, 2/\sqrt{3})$ to $(2\pi/a)(1/2, 5/2\sqrt{3})$. Those are not parallel to that of incident wave and the coupling may be small. Therefore the low transmittance corresponding to the range between the second and the seventh band may be caused by the wavevector mismatch between the external wave and the fourth and fifth bands which belong to the A representation, and non-coupling effect between the external wave and the third and sixth bands which belong to the B representation.

On the other hand, in the Γ - J direction we should not expect the low transmittance region corresponding to frequency between the second and seventh bands in spite that in this region the wavevector mismatch may take place. Because the Γ - J direction is parallel to that of J - X direction. (Fig. 7) For both polarizations of J - X direction there exist the third and fourth bands whose wavevectors of dominant plane-wave components in eigen-function are on the lines from $(2\pi/a)(2/3,0)$ to $(2\pi/a)(1,0)$ and from $(2\pi/a)(-4/3,0)$ to $(2\pi/a)(-1,0)$, respectively, and are parallel to that of the incident external wave. Therefore we can find the relatively high transmittance in the relevant region in the Γ - J direction. The frequencies of regions with low transmission and frequencies between relevant bands are listed on Table III.

Thus, we can explain all regions with quite low transmittance observed in the transmission spectra by means of the band gaps, non-coupling and wavevector mismatch.³¹

6 Conclusion

We fabricated two kind of photonic lattices with the lattice constant of $170 \mu\text{m}$ composed of triangular array or square array of circular air-rods with the average diameter of $105 \mu\text{m}$ and $95 \mu\text{m}$, respectively. The comparison of the observed transmission spectra in far-infrared region with the calculated band structure gave clear evidence for the existence of the uncoupled mode in both lattices in addition to the good correspondence of the opaque spectral ranges with the gap frequencies. Otherwise, the spectral regions with very low transmittance were also observed. In those regions there exist bands belonging to the A representation, whose dominant plane-wave component in eigen-function has the wavevector not parallel to the direction of propagating incident external wave, as well as the bands belonging to the B representation. We point out the possibility that the low transmittance is caused by the "wavevector mismatch".

Acknowledgements

The authors express their sincere thanks to Prof. K. Inoue and Prof. K. Sakoda of Hokkaido University and Prof. J. W. Haus and Dr. Z. Yuan of Rensselaer Polytechnic Institute for their valuable and stimulating discussions. Thanks are also due to Prof. H. Miwa of Shinshu University for their valuable discussions for the band structures. They appreciate to Dr. H. Matsuo of Nobeyama Radio Observatory and Drs. S. Nishizawa and K. Shirawachi of JASCO for helpful advises of the far-infrared measurements. This work was partly supported by Grant of Aid for Scientific Research of Priority Areas, "Mutual Quantum Manipulation" and by Grant of Aid for General Scientific Research of Ministry of Education, Culture of Japan.

References

- 1 K. Ohtaka, Phys. Rev. **B19**, 5057 (1979).
- 2 E. Yablonovich, Phys Rev. Lett. **58**, 2059 (1987).
- 3 E. Yablonovich, T. J. Gmitter, and K. M. Leung, Phys Rev. Lett. **67**, 2295 (1991).
- 4 E. Yablonovich and T. J. Gmitter, Phys Rev. Lett. **67**, 3380 (1991).
- 5 For a review see the articles in "*Photonic Band Gaps and Localization*" edited by C. M. Soukoulis (Plenum, New York 1993).
- 6 J. D. Joannopoulos, R. D. Meade and J. N. Winn, "*Photonic Crystals*" (Plinston, New Jersey 1995).
- 7 Special review issues [C. W. Bowden, J.P. Dowling, and H. O. Everitt, J. Mod. Opt. **41**, (1994)].
- 8 Special review issues [G. Kurizuki and J. W. Haus, J. Opt. Soc. Am. **B10**, (1993)].
- 9 G. Kurizki and A. Z. Genack, Phys Rev. Lett. **61**, 2269 (1988).
- 10 A. Z. Genack and N. Garcia, Phys Rev. Lett. **66**, 2064 (1991).
- 11 S. John and J. Wang, Phys. Rev. **B43**, 12772 (1991).
- 12 R. D. Meade, K. D. Brommer, A. M. Rappe, and J. D. Joannopoulos, Appl. Phys. Lett. **61**, 495 (1992).
- 13 W. M. Robertson, G. Arjavalingam, R. D. Meade, K. D. Brommer, A. M. Rappe, and J. D. Joannopoulos, Phys. Rev. Lett. **68**, 2023 (1992) and J. Opt. Soc. Am. **B10**, 322 (1993).
- 14 S. L. McCall, P. M. Platzman, R. Dalichaouch, D. Smith, and S. Schultz, Phys. Rev. Lett. **67**, 2017 (1991).
- 15 A. G. Kalocsai and J. W. Haus, Opt. Commun. **97**, 239 (1993).
- 16 M. Scalora, M. Tocci, M. Bloemer, C. M. Bowden, and J. W. Haus, Appl. Phys. **B60**, 557(1995).
- 17 P. R. Villeneuve and M. Piche, Phys. Rev. **B46**, 4969 (1992).
- 18 Plihal and A. A. Maradudin, Phys. Rev. **B44**, 4969 (1991).
- 19 K. M. Ho, C. T. Chan, and Soukoulis, Phys. Rev. Lett. **65**, 3152 (1990).
- 20 E. Ozbay, E. Michel, G. Tuttle, R. Biswas, K. M. Ho, J. Bastak, and D. M. Bloom, Appl. Phys. Lett. **65**, 1466 (1994).
- 21 S. Fan, P. R. Villeneuve, R. D. Meade, and J. D. Joannopoulos, Appl. Phys. Lett. **65**, 1466 (1994).
- 22 U. Gruning, V. Lehmann, and C. M. Engelhardt, Appl. Phys. Lett. **66**, 3254 (1995).
- 23 K. Inoue, M. Wada, K. Sakoda, A. Yamanaka, M. Hayashi, and J. W. Haus, Jpn. J. Appl. Phys. **33**, L1463 (1994).
- 24 K. Inoue, M. Wada, K. Sakoda, M. Hayashi, T. Fukutama, and A. Yamanaka, Phys. Rev. **B53**, 1010 (1996).
- 25 K. Sakoda, Phys. Rev. **B51**, 4672 (1995).
- 26 K. Sakoda, Phys. Rev. **B52**, 7982 (1995).
- 27 M. Wada, K. Sakoda, and K. Inoue, Phys. Rev. **B52**, 16297 (1995).
- 28 K. Sakoda, private communications.
- 29 M. Wada, K. Shirawachi, and S. Nishizawa, Jpn. J. Appl. Phys. **30**, 1122 (1991).
- 30 H. Miwa, private communications.
- 31 M. Wada, Y. Doi, K. Inoue, and J. W. Haus, Phys. Rev. **B55** (1997) in press.